Neutrosophic Logic Empowered Machine Learning Algorithm with Salp Swarm Optimization for Biomedical Image Analysis

Adwan A. Alanazi[1], Abdelgalal O. I. Abaker[2,*], Sayed Abdel-Khalek[3], Fahad Mohammed Alhomayani[4,5], M. Aripov[6]

[1]Department of Computer Science and Information, University of Hail, Saudi Arabia
[2]Applied College, Khamis Mushait, King Khalid University, Abha, Saudi Arabia
[3]Department of Mathematics and Statistics, College of Science, Taif University, P. O Box 11099, Taif 21944, Saudi Arabia
[4]College of Computers and Information Technology, P.O. Box 11099, Taif University, Taif 21944, Saudi Arabia
[5]Applied College, P.O. Box 11099, Taif University, Taif 21944, Saudi Arabia
[6,1]Department of Applied Mathematics and Computer Analysis, Faculty of Mathematics, NUU, Uzbekistan
Emails: a.alanazi@uoh.edu.sa; aoadrees@kku.edu.sa; sayedquantum@yahoo.co.uk; fahad@tu.edu.sa; aripovmersaid@gmail.com
[*]Corresponding Author: aoadrees@kku.edu.sa

Abstract

Leukemia recognition and classification contain the identification of dissimilar kinds of leukemia, a group of blood cancers that affects the bone marrow and blood. A classical model containing microscopic analysis of blood smears to classify abnormal cells analytic of leukemia. Leukemia recognition employing a united technique of neutrosophic logic and deep learning (DL) signifies a new and complete approach to handling uncertainty and difficulty in medical data. Neutrosophic logic permits the representation of unstated or imperfect data, which is general in medical analyses. DL mainly convolutional neural networks (CNN) or recurrent neural networks (RNN), which can mechanically remove difficult patterns from medicinal imageries, improving the accuracy of leukemia recognition. The neutrosophic logic module accommodates the characteristic uncertainty in medicinal data, offering a formalism to manage imperfect or inaccurate data linked with the analysis procedure. The combination of these dual techniques generates a robust structure which capable of leveraging both the control of DL in image analysis and the flexibility of neutrosophic logic in dealing with uncertainties, contributing to more trustworthy and interpretable leukemia recognition methods. This study develops a new Salp Swarm Algorithm with a Neutrosophic Logic SVM (SSA-NSVM) model for Leukemia Detection and Classification. The SSA-NSVM technique mainly exploits Neutrosophic Logic (NL) concepts with the DL model for the detection of leukemia. To attain this, the SSA-NSVM model uses bilateral filtering (BF) based image pre-processing. In addition, the SSA-NSVM approach applies a modified densely connected networks (DenseNet) technique for learning complex and intrinsic feature patterns. Besides, the hyperparameter range of the modified DenseNet system takes place utilizing a SSA. At last, the NSVM technique is employed for the detection and identification of leukemia. The performance validation of the SSA-NSVM algorithm is verified utilizing a benchmark medicinal image dataset. The simulation values emphasized that the SSA-NSVM model reaches better detection outcomes than other existing approaches.

Keywords: Leukemia Detection; Neutrosophic Logic; Bone Marrow; Salp Swarm Algorithm; Blood Cancer

1. Introduction

Leukemia is a kind of blood cancer that originates in the bone marrow leads to a huge amount of unusual blood cells [1] are commonly named leukemia or blast cells cannot able to fully develop. The potential signs like bone distress, bleeding, weariness, bruising, fever, and a high danger of infection. A lack of normal blood cells causes such kind of indications. Blood analysis or bone marrow biopsy must be generally utilized to execute the identification [2]. The

Doi: https://doi.org/10.54216/IJNS.230408
Received: August 02, 2023 Revised: December 04, 2023 Accepted: March 01, 2024

real reasons for leukemia may be unrecognized by researchers. It performs to be the effect of a combination of genetic and environmental aspects. A major problem in the domain of disorder analysis is the exact discrepancy of malignant leukocytes with lower cost at the earlier phases of the illness to be more complex [3]. Generally, leukemia analysis can be separated into two types: translational or clinical and basic research. Translational or clinical research considers reviewing disease in a particular and directly appropriate way like testing the new drugs in humans [4]. Alternatively, the research analyses the disease method like whether a suspicious carcinogen will cause the leukemic variations in separated cells in the lab [5]. While microscopic analysis of PBS is a major prevalently employed technique for diagnosing leukemia, gaining and testing bone marrow biopsy becomes the gold standard for leukemia identification. In recent times, proficient systems to analyze tumorous gene data are improving, and machine learning (ML) methods have been presently employed [6]. ML will support intelligence and automated methods, increase development, accuracy, and minimize expenses [7]. During the past years, numerous researchers have employed ML and computer-aided diagnosis (CAD) techniques for laboratory image study, supporting to address the restrictions of a final stage leukemia analysis and identifying its subcategories [8]. The researcher workers have examined blood smear images for analyzing, counting, and distinguishing the cells in diverse categories of leukemia. ML is a popular subdivision of artificial intelligence (AI), encompassing methods and mathematical correlations that are rapidly presented to the field of medical examination [9]. ML permits computers to be automated without clear involvement and learns from that familiarity. ML ensemble techniques and deep learning (DL) are indicated higher effective for categorizing biological data [10].

This study develops a new Salp Swarm Algorithm with a Neutrosophic Logic SVM (SSA-NSVM) model for Leukemia Detection and Classification. The SSA-NSVM technique mainly exploits Neutrosophic Logic (NL) concepts with the DL model for the detection of leukemia. To complete this, the SSA-NSVM system initially uses bilateral filtering (BF) based image pre-processing. In addition, the SSA-NSVM approach applies a modified densely connected networks (DenseNet) method for learning complex and intrinsic feature patterns. Also, the hyperparameter range of the modified DenseNet sytem takes place utilizing SSA. At last, the NSVM method is used for the detection and identification of leukemia. The performance validation of the SSA-NSVM method is verified utilizing a benchmark medical image dataset.

2. Literature Review

Talaat and Gamel [11] proposed an innovative classification method. The developed technique involves three major stages namely (1) Feature Extraction, (2) Image_Preprocessing, and (3) Classification. An optimized-Convolution Neural Network (OCNN) was employed for classification. OCNN has been employed for identifying and categorizing the image as normal or abnormal. A fuzzy optimizer was employed to enhance the hyperparameter of CNN. Still, it is advantageous to utilize fuzzy logic (FL) in the OCNN. Sriram et al. [12] intended to automate the method employing ML. Primarily, automated detection and calculating of WBC has been achieved. VGG16 and CNN model-based DL methods were integrated for categorization and counting WBC categories at segmented images. Jha et al. [13] examined a wide-ranging analysis of automatic acute lymphoblastic leukemia (ALL) identification methods employing image processing and artificial intelligence (AI) methods. In ML–based techniques, features of blood smear images have been removed individually however, this stage is not needed in DL–based techniques. For images from the ALL-IDB, classification outcomes of various methods have been evaluated.

Elrefaie et al. [14] presented an enhanced standard for categorizing ALL microscopic images. Primarily, innovative image preprocessing methods have been utilized. The K-means clustering technique could be also employed for segmentation. Similarly, the noticeable features must be removed by employing an empirical mode decomposition (EMD) dependent upon the Hilbert-Huang conversion. MATLAB tasks have been employed and related. The Bayesian regularization (BR) technique was deployed in the neural networks (NNs). By utilizing NNs, alternative machine algorithms should be employed, assessed, and contrasted with NNs. Das et al. [15] implemented an innovative and efficient method. A new Orthogonal SoftMax Layer (OSL)-based Acute Leukemia recognition technique that includes ResNet18-based deep feature extractor after that effective OSL-based classification has been developed. The OSL can be combined with the ResNet18 for categorization. Therefore, it incorporates ResNet advantages (identity mapping and residual learning) with the advantages of OSL-based classification. Also, additional dropout and ReLU layers have been presented for the model.

Bhute et al. [16] developed an ensemble learning-based techniques. Ensemble learning was employed for determining patterns and predicting the existence of the disease. Various pre-trained techniques have been deployed in this work for recognized diverse types of leukemia. Pretrained architectures like InceptionV3, VGG16, and ResNet50 could be moderately simple methods for implementing ensemble learning to image analysis, and thus, they can be enhanced for feature extraction and classification. In [17], a deep feature selection (FS)-based technique ResRandSVM was developed. This technique employs 7 DL methods such as ResNet50, VGG16, ResNet152, InceptionV3,

Doi: https://doi.org/10.54216/IJNS.230408
Received: August 02, 2023 Revised: December 04, 2023 Accepted: March 01, 2024

DenseNet121, MobileNetV2, and EfficientNetB0 for deep feature extraction. Next, Random Forest (RF), analysis of variance (ANOVA), and principal component analysis (PCA) are the three FS methods have been employed for the extraction. In conclusion, the chosen feature map was provided a 4 various methods for classification.

3. Neutrosophic Sets

Here, the neutrosophic set is presented with their fundamental notions and properties with illustrative example [18].
Definition 2.1.1: Consider a universe of discourse as N and a neutrosophic set A on N is described by the following equation:

$$A = \{\langle n, T_A(n), I_A(n), F_A(n)\rangle, n \in N\}$$

Here $T, I, F: N \rightarrow]^{-}0, 1^{+}[$ and $-0 \leq T_A(n) + I_A(n) + F_A(n) \leq 3^{+}$.
From philosophical perspective, neutrosophic set take the value within $[0,1]$, since it is challenging to apply neutrosophic set with non-standard or real standard subset of $]^{-}0, 1^{+}]$.
Definition 2.1.2: A neutrosophic set A is confined in other neutrosophic sets B, if
$T_A(n) \leq T_B(n), I_A(n) \leq I_A(n), F_A(n) \geq F_B(n)$ for all $n \in N$.
Definition 2.1.3: An component x of U is named significant regarding neutrosophic set A of U when the degree of falsity-membership or indeterminancy-membership or truth-membership values, viz., $F_{A(n)}$ or $I_{A(n)} or\ T_{A(n)} \leq 0.5$.
If not, we call it insignificant. Also, falsity-membership and indeterminacy-membership is not crucial for the neutrosophic set and the truth-membership:
$A = \{< n: T_{A(n)}, I_{A(n)}, F_{A(n)} >, n \in U\}$, where $\min\{T_{A(n)}, F_{A(n)}\} \leq 0.5$, $\min\{T_{A(n)}, I_{A(n)}\} \leq 0.5$, $\min\{F_{A(n)}, I_{A(n)}\} \leq 0.5$, for all $n \in U$, with the condition $0 \leq T_{A(n)} + I_{A(n)} + F_{A(n)} \leq 2$.
Example 2.1.4: Consider $U = \{n_1, n_2, n_3\}$, where n_1 denotes the ability, n_2 symbolizes the trustworthiness and n_3 specifies the object prices. Furthermore, consider that the value of n_1, n_2 and n_3 within [0,1] and they are attained from some questionnaire of certain expert. Assume A as an intuitionistic neutrosophic set (IN S) of U,

$$A = \{< n_1, 0.3, 0.5, 0.4 >, < n_2, 0.4, 0.2, 0.6 >, < n_3, 0.7, 0.3, 0.5 >\},$$

Where the degree of falsity of ability is 0.4, degree of goodness of ability is 0.3, and degree of indeterminacy of ability is 0.5 and so on.
Definition 2.1.5: Consider N is a objects with generic components in N represented as n. A neutrosophic set A in N is represented as a indeterminacy membership function $I_A(n)$, a falsity membership function $F(n)$, and a truth-membership function $T_A(n)$ if the function $I_A(n)$, $F_A(n)$, $T_A(n)$ are singletons subsets or subintervals in the real standard $[0,1]$, viz., $I_A(n): N \rightarrow [O, 1]$, $F_A(n): N \rightarrow [O, 1]]$, $T_A(n): N \rightarrow [0,1]$. Next, the neutrosophic set A is represented as $A = \{< n: T_A(n), I_A(n), F_A(n) >, n \in N\}$.
Definition 2.1.6: Assume N as a objects with generic components in N represented as n. An SVNS A in N is represented as a truth-membership function T_A, an indeterminacy membership function $I_A()$ and a falsity-membership function for all the points $n \in N, T_A(n)$, $I_A(n)$, $F_A(n) \in [0,1]$. Thus, a SVNS A is formulated by $A_{SVNS} = \{< n: T_A(n), I_A(n), F_A(n) >, n \in N\}$.
For two SVNS, $A_{SVNS} = \{< n: T_A(n), I_A(n), F_A(n) >, n \in N\}$ and $B_{SVNS} = \{< n: T_B(n), I_B(n), F_B(n) >, n \in N\}$, the subsequent formula is described by,
$A_{NS} \subseteq B_{NS}$ if and only if $T_A(n) \leq T_B(n), I_A(n) \geq I_B(n), F_A(n) \geq F_B(n)$. $A_{NS} = B_{Ns}$ if and only if $T_A(n) = T_B(n)$, $I_A(n) = I_B(n), F_A(n) = F_B(n)$. $A^c =< n, F_A(n), 1 - I_A(n), T_A(n) >$
SVNS A is represented as $A =< T_A(n), I_A(n)\ F_A(n) >$ for any $n \in N$; for two SVNSs A and B. Then,
(1) $\cup\ B =<$ max $(T_A(n), T_B(n))$, $\min(I_A(n), I_B(n), \min(T_A(n), T_B(n)) >$
(2) $\cap\ B =<$ min $(T_A(n), T_B(n))$, $\max(I_A(n), I_B(n), \max(T_A(n), T_B(n)) >$

4. The Proposed Method

In this paper, we have presented a novel SSA-NSVM procedure for leukemia recognition and identification. The SSA-NSVM approach mainly exploits NL concepts with the DL model for the detection of leukemia. It comprises different kinds of sub-processes such as BF-based preprocessing, DenseNet-based feature extractor, SSA-based hyperparameter selection, and NSVM-based classification process. Fig. 1 demonstrates the entire procedure of the SSA-NSVM model.

Doi: https://doi.org/10.54216/IJNS.230408
Received: August 02, 2023 Revised: December 04, 2023 Accepted: March 01, 2024

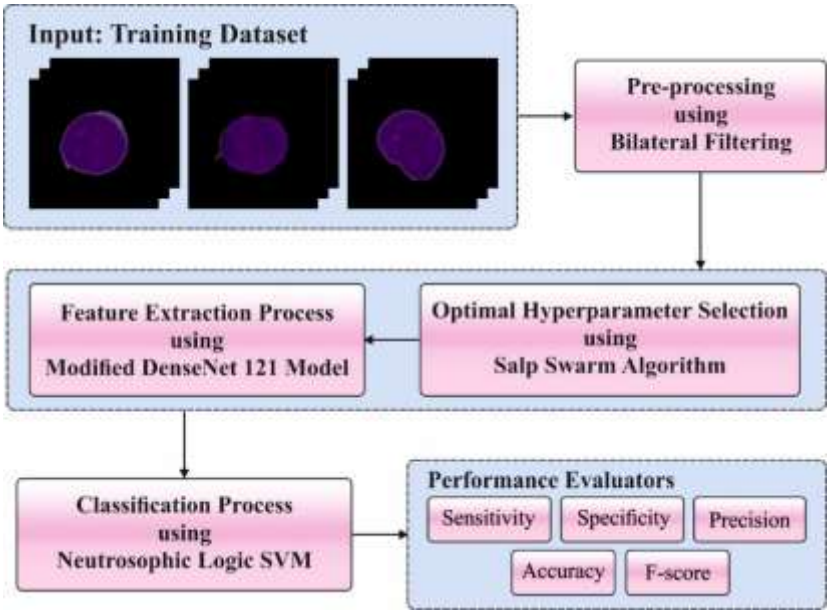

Figure 1: Overall process of SSA-NSVM model

A. Image Pre-processing

Initially, the SSA-NSVM approach uses BF-based image pre-processing. BF aids as a great device to improve the excellence of medicinal imageries by efficiently decreasing noise while maintaining vital structural particulars and edges [19]. By striking a balance between noise suppression and edge protection, BF guarantees that refined features indicative of leukemia cells are precisely taken and emphasized. This refined pre-processing stage plays an essential part in enhancing later analysis and classification models, offering them clean and useful input data. The flexibility of bilateral filtering permits customization to fluctuating imaging states, further strengthening its value in leukemia analysis. Its dual-domain technique considers both spatial proximity and strength resemblance and permits exact feature extractor which is crucial for accurate recognition. By refining input data, BF authorizes ML techniques to distinguish subtle patterns and features of leukemia cells, finally foremost to more reliable diagnosis and classification results.

B. DenseNet Model

The SSA-NSVM technique uses a modified DenseNet model for learning complex and intrinsic feature patterns. DenseNet121 comprises several dense blocks, each one comprises of several convolution layers [20]. Inside all the dense blocks, the input to all the convolution layers is the concatenation of the mapping feature of every preceding layer. This densely linked structure creates DenseNet to carry out optimum feature reprocessing, efficiently decreasing the number of parameters and enhancing the entire computation effectiveness. Besides, this structure also supports improving the vanishing gradient problem.

$$X_l = H_l([X_0, X_1, \dots, X_{l-1}]), \quad (1)$$

Whereas, X_l defines the mapping feature. $[X_0, X_1, \dots, X_{l-1}]$ signifies the mapping feature that is linked to the layer and $H_l(\cdot)$ stands for the composite function that comprises rectified linear units (ReLU), batch normalization (BN), and convolutional.

Conversely, as the layer counts of the network develop deeper, the channel counts progress superior, and the parameter counts develop greater which creates it complex to train a deeper system. Accordingly, DenseNet also comprises a vital Transition Layer for connecting 2 dense blocks. The layer of transition decreases the channel counts of the acquired mapping feature to half of the new and carries out downsampling to split the size, making simpler the computation and enhancing the computation effectiveness.

Doi: https://doi.org/10.54216/IJNS.230408
Received: August 02, 2023 Revised: December 04, 2023 Accepted: March 01, 2024

Layers	Output Size	DenseNet-121	DenseNet-169	DenseNet-201	DenseNet-264
Convolution	112 × 112	7 × 7 conv, stride 2			
Pooling	56 × 56	3 × 3 max pool, stride 2			
Dense Block (1)	56 × 56	[1 × 1 conv, 3 × 3 conv] × 6	[1 × 1 conv, 3 × 3 conv] × 6	[1 × 1 conv, 3 × 3 conv] × 6	[1 × 1 conv, 3 × 3 conv] × 6
Transition Layer (1)	56 × 56	1 × 1 conv			
	28 × 28	2 × 2 average pool, stride 2			
Dense Block (2)	28 × 28	[1 × 1 conv, 3 × 3 conv] × 12	[1 × 1 conv, 3 × 3 conv] × 12	[1 × 1 conv, 3 × 3 conv] × 12	[1 × 1 conv, 3 × 3 conv] × 12
Transition Layer (2)	28 × 28	1 × 1 conv			
	14 × 14	2 × 2 average pool, stride 2			
Dense Block (3)	14 × 14	[1 × 1 conv, 3 × 3 conv] × 24	[1 × 1 conv, 3 × 3 conv] × 32	[1 × 1 conv, 3 × 3 conv] × 48	[1 × 1 conv, 3 × 3 conv] × 64
Transition Layer (3)	14 × 14	1 × 1 conv			
	7 × 7	2 × 2 average pool, stride 2			
Dense Block (4)	7 × 7	[1 × 1 conv, 3 × 3 conv] × 16	[1 × 1 conv, 3 × 3 conv] × 32	[1 × 1 conv, 3 × 3 conv] × 32	[1 × 1 conv, 3 × 3 conv] × 48
Classification Layer	1 × 1	7 × 7 global average pool			
		1000D fully-connected, softmax			

Figure 2: Architecture of DenseNet121

The presented technique exploits an enhanced version of the DenseNet121 model. This architecture includes a change in network parameters and meta-parameter. Fig. 2 demonstrates the framework of the DenseNet121 model.

As a piece-wise linear task, Rectified linear unit (ReLu) directly yields the input or else, it produces 0. It improves network performance, although adding an activator function occupies more of the computation memory and increases the volume of calculation. Moreover, the ReLu function doesn't eliminate the negative portion, which learns more features through the network and causes a superior movement of gradients. According to Eq. (2), we mathematically defined Mish, as a non-monotonic activation function.

$$f(x) = xtanh\big(ln(1 + e^x)\big) \quad (2)$$

When compared to the ReLu function, the Mish activation function better enhances the DL performance. The network parameter differs from the function of ReLu and is replaced with M function of activation. Stochastic gradient descent with momentum (SGDM) technique helps speed up gradient vector to accomplish fast converging. Instead of using only the gradient of the existing step, The SGDM approach acquires the gradient of the prior step to define the direction. Rectified Adam (RAdam) is a special type of Adam optimizer to resolve the alteration of the adaptive rate of learning. The essential characteristics of the RAdam optimizer are high accuracy and fast convergence. The changes made in the network meta-parameter are to use RAdam and change the SGDM optimizer.

C. Hyperparameter Tuning using SSA

In this study, the hyperparameter range of modified DenseNet model takes place by employing SSA. The SSA describes a bio-inspired algorithm [21]. Salps are marine organisms characterized by the Salpidae family, with a luminous barrel-structured body that can be nearly similar to jellyfish. They are moving the same as jellyfish, utilizing their body to drive water for momentum. While technical exploration on salps is quiet at earlier phases, their swarming behavior is the most attractive feature of the types. Salps frequently procedure a swarm that is termed a salp chain from deep waters like oceans. Although the correct causes for this behavior were unidentified, a few research workers believe it is employed for increasing movement via synchronized modifications and searching. The exclusive features of salps must stimulate the improvement of the SSA method that imitates the swarming behavior of salps for resolving optimizer difficulties. It has revealed excellent outcomes in different optimization tasks because of its capability for balancing exploration and exploitation. However, additional researches are required to comprehend and apply the complete perspective of the SSA technique.

The subsequent steps reviewed the fundamental stages of the original SSA:

1. Parameters Initialization.

This stage of SSA includes producing an early population of candidate solution in which every solution. This initialization stage usually involves arbitrarily allocating that makes an initial set of candidate solution. Then it is assessed through fitness function (FF) like the Addition of Squared Error (SSE) that calculates the excellence of the solution. The candidate solution have been categorized dependent on their fitness, and the fittest decision will be chosen for producing the subsequent production of candidate solution. To increase the variety of the populace, SSA implements a local search process that troubles the fittest outcomes for determining the neighboring search space. The

Doi: https://doi.org/10.54216/IJNS.230408
Received: August 02, 2023 Revised: December 04, 2023 Accepted: March 01, 2024

operator of a local search supports avoiding untimely convergence and improving the probabilities of identifying good solutions. The initialization stage of SSA performs a vital function to find the quality of the last result. A well-developed initialization stage could produce different collections of candidate solution. It raises the probability of determining a higher-quality result and enhancing the method's rate of convergence.

2. The Salp Chains architecture.

In this stage, the SSA comprises categorizing the solutions into binary types such as followers and leaders that are dependent upon their main function values. The leader set will be positioned in front of the salp chain to manage the alternative decision. The populace of solution should be denoted as a 2D matrix in which every row signifies many solutions, and all solutions exist as a d-dimension vector. Now, the variable d denotes dimension for the optimizer difficulty (Eq. 3). The leader set's location will be upgraded by applying Eq. (4), where c_2 and c_3 refers to random numbers, x_d^1 describes a leader solution, d defines the food source, $F(d)$ denotes the decision variable, and c_1 refers to a coefficient measured by Eq. (5). The follower set's solutions have been updated by applying Eq. (6), where x_d^{m-1} and x_d^m describes the d^{th} dimension of the prior and existing solution at iteration $m-1$ and m, respectively. This SSA method upgrades solutions in its implementation for exploring the search space of the optimizer difficulties according to the search tactic of the method.

$$SSAM = \begin{bmatrix} x_1^1 & x_2^1 & \dots & x_d^1 \\ x_1^2 & x_2^2 & \dots & x_d^2 \\ \vdots & \vdots & \dots & \vdots \\ x_1^m & x_2^m & \dots & x_d^m \end{bmatrix}. \quad (3)$$

$$x_d^1 = \begin{cases} \lfloor F(d) + c_1 \times \left((ub_d - lb_d) \times c_2 + lb_d\right) \rfloor \\ c3 \geq 0, \\ \lfloor F(d) - c_1 \times \left((ub_d - lb_d) \times c_2 + lb_d\right) \rfloor \\ c3 < 0 \end{cases} \quad (4)$$

$$c_1 = 2 \times exp - \left(\frac{4l}{L_{\max}}\right)^2 \quad (5)$$

$$x_d^m = \frac{1}{2}(x_d^m + x_d^{m-1}) \quad (6)$$

Step 3:Stop condition.

At this stage, the performance of SSA (like stage 2) should be ended depending upon the quality of the last outcomes or accomplishment of the predetermined count of iterations.

The fitness function (FF) is the significant factor manipulating the performance of SSA. The hyperparameter range method contains the solution encode technique to assess the effectiveness of the candidate solution. In this paper, the SSA considers accuracy as the foremost principle to project the FF that is conveyed as.

$$Fitness = \max(P) \quad (7)$$

$$P = \frac{TP}{TP + FP} \quad (8)$$

Here, TP and FP indicate the true positive value and false positive value, correspondingly.

D. NSVM-based Classification Process

Lastly, the NSVM method is used for the recognition and identification of leukemia. Set a training set S enclosing n considered points $(x_1, y_1), \dots, (x_n, y_n)$, whereas $x_j \in R^N$ and $y_j \in \{-1,1\}, j = 1, \dots, n$ [22]. Assume the negative and positive samples are divided by a hyperplane. SVM's purpose is to discover an optimum result by boosting the margin M near the splitting hyperplane that is equal to the decrease $\|w\|$ by the restraint:

$$y_j(w \cdot x_j + b) \geq 1 \quad (9)$$

The original samples cannot able to be divided by the hyperplane, then SVM convert the samples of the original into the highest dimension space by employing a non-linear map. Let $\Phi(x)$ represent the map from R^N to the highest dimension space Z. A hyperplane wants to originate in the highest dimension space with the highest border as:

$$w \cdot z + b = 0 \quad (10)$$

For every point (z_j, y_j), whereas $z_j = \Phi(x_j)$:

$$y_j(w \cdot z_j + b) \geq 1, j = 1, \dots, n. \quad (11)$$

If the database is not functionally separate, the soft border has been permitted by presenting n non-negative variable, signified by $= (\xi_1, \xi_2, \dots, \xi_n)$, so the restraint for every sample in Eq. (11) has been modified as:

$$y_j(w \cdot z_j + b) \geq 1 - \xi_j, j = 1, \dots, n. \quad (12)$$

The optimum hyperplane is the solution:

Doi: https://doi.org/10.54216/IJNS.230408
Received: August 02, 2023 Revised: December 04, 2023 Accepted: March 01, 2024

$$minimize\ \frac{1}{2}w \cdot w + C\sum_{j=1}^{k}\xi_j \tag{13}$$

$$subject\ to\ y_j(w \cdot z_j + b) \geq 1 - \xi_j, j = 1, \dots, n. \tag{14}$$

Where Eq. (13) evaluates the border among support vector, and the 2nd term assesses the number of mis-classifications. The constant variable C adjusts the balance among the highest margin and the lowest classifier error. Next, $\hat{x}$ is mapped to $\hat{z}$, the classification outcome $\hat{y}$ is assumed as:

$$\hat{y} = sign(w \cdot \hat{z} + b) \tag{15}$$

The neutrosophic set is a simplification of the fuzzy and traditional set. 1 The step of neutralities <Neut-A> is presented. Usually, a neutrosophic set is signified as $< T, I, F >$. A section $x(t, i, f)$ fits the set in the next method: it is f false, i indeterminate and t true; whereas $i, f, and\ t$ are real numbers that are captured from sets T, I, and F. Numerous investigation outcomes have revealed that the normal SVM is highly complex to outliers. At this point, a neutrosophic set for the input sample dependent upon the spaces among the class centers and sample is provides. When combined into the re-formulated SVM, the neutrosophic set aids in resolving the issues of outlier and discovers the 3D distribution of training sample. Input samples related to the definite neutrosophic set have been signified as a set of points $(x_j, y_j, t_j, i_j, f_j), j = 1, \dots, n$. For input sample x_j belongs to class y_j, it is t_j true, i_j indeterminate, and f_j false. The center of positive samples C_+, negative samples C_-, and all samples C_{a11} have been well-defined as below:

$$C_+ = \frac{1}{n_+}\sum_{k=1}^{n_+} x_k\,, C_- = \frac{1}{n_-}\sum_{k=1}^{n_-} x_k\,, C_{all} = \frac{1}{n}\sum_{k=1}^{n} x_k \tag{16}$$

Whereas n_- and n_+ denotes the amount of negative and positive samples, correspondingly.

We signify P, N, and U as the positive, negative, and complete input samples subset, respectively. For a positive sample, $y_j = 1$, the neutrosophic modules were certain as:

$$t_j = 1 - \frac{\|x_j - C_+\|}{\max_{x_k \in P}\|x_k - C_+\|}$$

$$i_j = 1 - \frac{\|x_j - C_{all}\|}{\max_{x_k \in U}\|x_k - C_{all}\|} \tag{17}$$

$$f_j = 1 - \frac{\|x_j - C_-\|}{\max_{x_k \in P}\|x_k - C_-\|}$$

where $\|x\|$ represents the Euclidean distance of x variable. For the negative sample, $y_j = -1$, the neutrosophic modules were definite as:

$$t_j = 1 - \frac{\|x_j - C_-\|}{\max_{x_k \in N}\|x_k - C_-\|}$$

$$i_j = 1 - \frac{\|x_j - C_{all}\|}{\max_{x_k \in U}\|x_k - C_{all}\|} \tag{18}$$

$$f_j = 1 - \frac{|\|x_j - C_+\|}{\max_{x_k \in N}\|x_k - C_+\|}$$

By the above descriptions, each input sample is linked with a threefold $< t_j, i_j, f_j >$ as its neutrosophic modules. The greater t_j has a higher probability so it fits into the considered class. The larger i_j has a greater probability it is unknown. The larger f_j has a bigger probability so it fits to the reverse of the considered class. The threefold comprises valued data removed from the 3-D distribution of the training sample and offers useful evidence in the classifier plan. A weight function for the input sample must be definite to employ the re-formulated SVM. Each sample is linked with a triple $< t_j, i_j, f_j >$ as its neutrosophic modules. A greater t_j indicates that the samples are closer to the midpoint of the considered class and lesser probable being an outlier. So, t_j must be highlighted in the weight function. A greater i_j signifies that the sample is harder to differentiate among dual classes. This feature must be highlighted in the weight function to classify the unknown samples more precisely. A greater f_j indicates that the sample is more probable to be an outlier. This model must be preserved less highly in the training process.

$$g_j = t_j + i_j - f_j \tag{19}$$

After combining the developed weight function into the re-formulated SVM, training samples are employed inversely in the training process as per their 3-D distribution. Therefore, the projected classifier is signified as NSVM, decreases the effects of outliers and enhances the solution when equated to a normal SVM.

Doi: https://doi.org/10.54216/IJNS.230408
Received: August 02, 2023 Revised: December 04, 2023 Accepted: March 01, 2024

5. Result Analysis

In this section, the leukemia recognition results of the SSA-NSVM approach is verified using the image database from the Kaggle repository [23]. The database includes 4000 samples with dual classes as definite in Table 1. Fig. 2 exhibits the sample images.

Table 1: Details on database

Classes	No. of Instances
Leukemia	2000
Normal	2000
Total Instances	4000

The classifier outcomes of the SSA-NSVM system below the dual database is shown in Fig. 3. Figs. The confusion matrices provided by the SSA-NSVM technique on 70:30 of TRAS/TESS is demonstrated in 3a-3b. The figure indicated that the SSA-NSVM model has familiar and classified all 2 class labels exactly. Similarly, the PR research of the SSA-NSVM system is revealed in Fig. 3c. The figure defined that the SSA-NSVM method has gotten the maximum PR performance under all classes. Lastly, the ROC study of the SSA-NSVM approach is established in Fig. 3d. The figure depicts that the SSA-NSVM model has resulted in proficient outcomes with maximum ROC values under different classes.

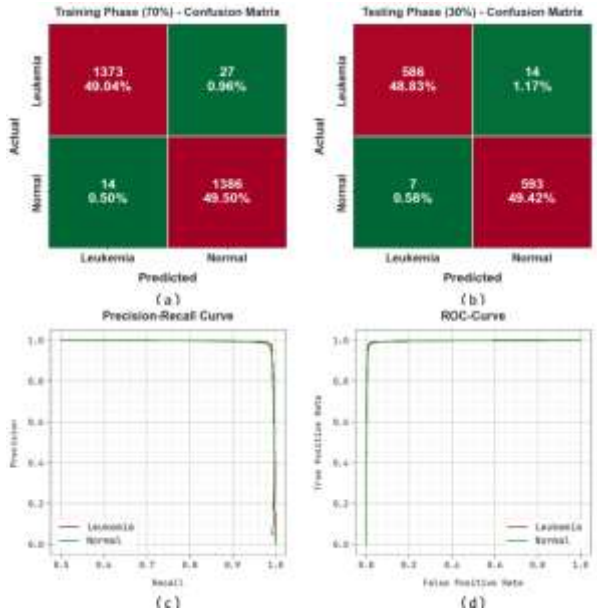

Figure 3: Classifier outcomes of (a-b) Confusion matrices and (c-d) PR and ROC curves

The leukemia recognition outcomes of the SSA-NSVM technique are conveyed in Table 2 and Fig. 4. The outcomes outlined that the SSA-NSVM system appropriately identified the normal and leukemia samples. With 70%TRAS, the SSA-NSVM system gets an average $accu_y$ of 98.54%, $prec_n$ of 98.54%, $sens_y$ of 98.54%, $spec_y$ of 98.54%, and F_{score} of 98.54%. Also, with 30%TESS, the SSA-NSVM system gains average $accu_y$ of 98.25%, $prec_n$ of 98.26%, $sens_y$ of 98.25%, $spec_y$ of 98.25%, and F_{score} of 98.25%.

Table 2: Leukemia recognition outcomes of the SSA-NSVM approach under 70:30 of TRAS/TESS

Classes	$Accu_y$	$Prec_n$	$Sens_y$	$Spec_y$	F_{Score}
TRAS (70%)					
Leukemia	98.07	98.99	98.07	99.00	98.53
Normal	99.00	98.09	99.00	98.07	98.54
Average	98.54	98.54	98.54	98.54	98.54
TESS (30%)					
Leukemia	97.67	98.82	97.67	98.83	98.24
Normal	98.83	97.69	98.83	97.67	98.26
Average	98.25	98.26	98.25	98.25	98.25

Doi: https://doi.org/10.54216/IJNS.230408
Received: August 02, 2023 Revised: December 04, 2023 Accepted: March 01, 2024

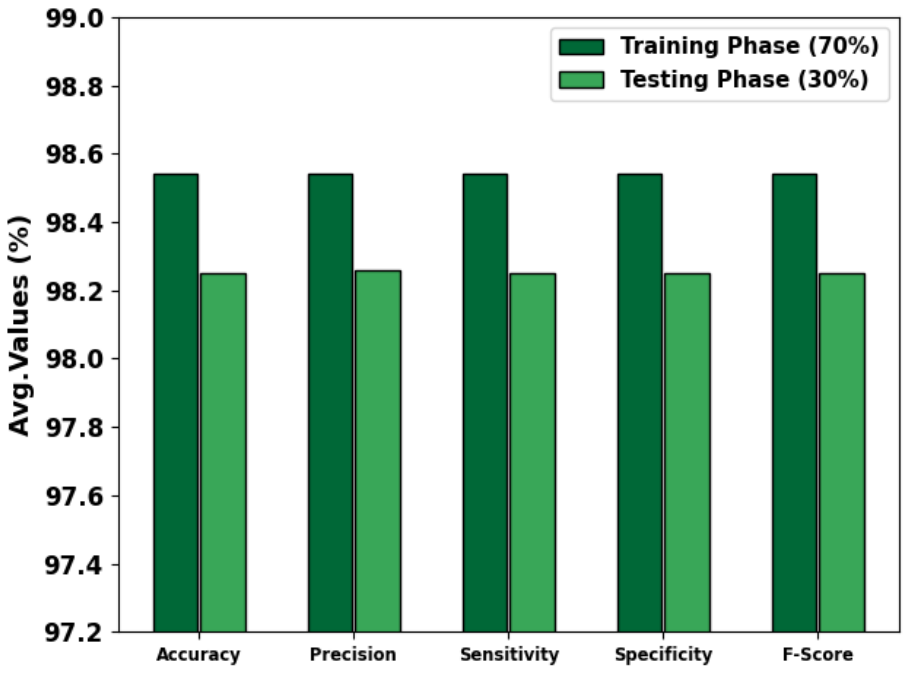

Figure 4: Average of SSA-NSVM method on 70:30 of TRAS/TESS

The performance of the SSA-NSVM technique is offered in Fig. 5 in the procedure of training accuracy (TRAA) and validation accuracy (VALA) curves. The figure displays beneficial clarification into the performance of the SSA-NSVM model over some epoch count, representing its learning procedure and generalized skills. Remarkably, the figure concludes a stable improvement in the TRAA and VALA with development in epochs. It certifies the adaptive nature of the SSA-NSVM system in the pattern detection method on both TRA and TES data. The rising trend in VALA summarizes the ability of the SSA-NSVM system on familiarizing to the TRA data and also excels in providing a precise classification of hidden data, indicating robust generalized skills.

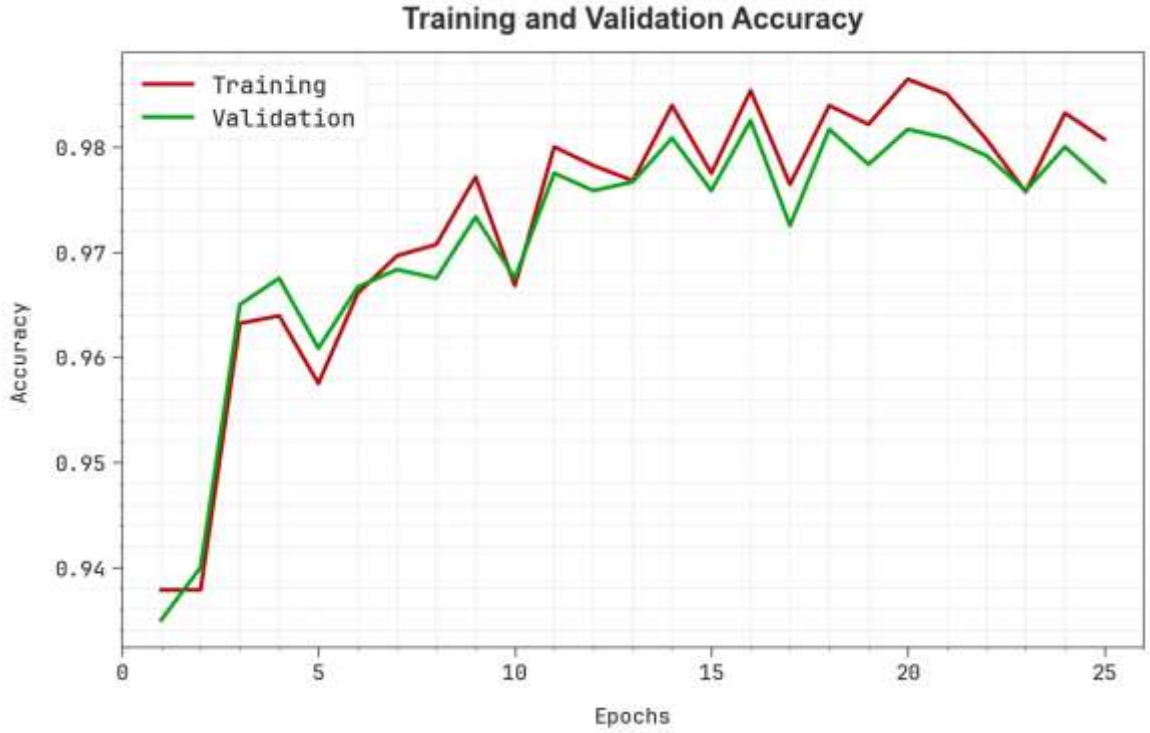

Figure 5: $Accu_y$ curve of the SSA-NSVM approach

Doi: https://doi.org/10.54216/IJNS.230408
Received: August 02, 2023 Revised: December 04, 2023 Accepted: March 01, 2024

In Table 3 the outcomes of the SSA-NSVM system is compared with other ones [11, 24]. Fig. 6 offers a comparison analysis of the SSA-NSVM method in terms of $prec_n$ and $accu_y$. The figure illustrated that the SSA-NSVM approach gains increased performance. Based on $prec_n$, a higher value of 98.54% is accomplished by the SSA-NSVM technique whereas the CNN, SVM-linear, KNN, DT, ResNet, and MobileNet models have reported lower $prec_n$ of 93.62%, 97.21%, 92.97%, 95.69%, 95.50%, and 89.70%, correspondingly. Additionally, based on $accu_y$, a higher value of 98.54% is accomplished by the SSA-NSVM system whereas the CNN, SVM-linear, KNN, DT, ResNet, and MobileNet techniques have stated lower $accu_y$ of 92.37%, 97.68%, 92.47%, 95.82%, 96%, and 97%, respectively.

Table 3: Comparative analysis of the SSA-NSVM technique with existing methods

Performance	$Prec_n$	$Sens_y$	$Accu_Y$	$Spec_y$
SSA-NSVM	98.54	98.54	98.54	98.54
CNN Model	93.62	93.38	92.37	90.38
SVM-Linear	97.21	90.89	97.68	91.54
KNN Algorithm	92.97	92.52	92.47	95.99
DT Model	95.69	95.96	95.82	95.67
ResNet50	95.50	96.10	96.00	90.20
MobileNet	89.70	97.50	97.00	88.10

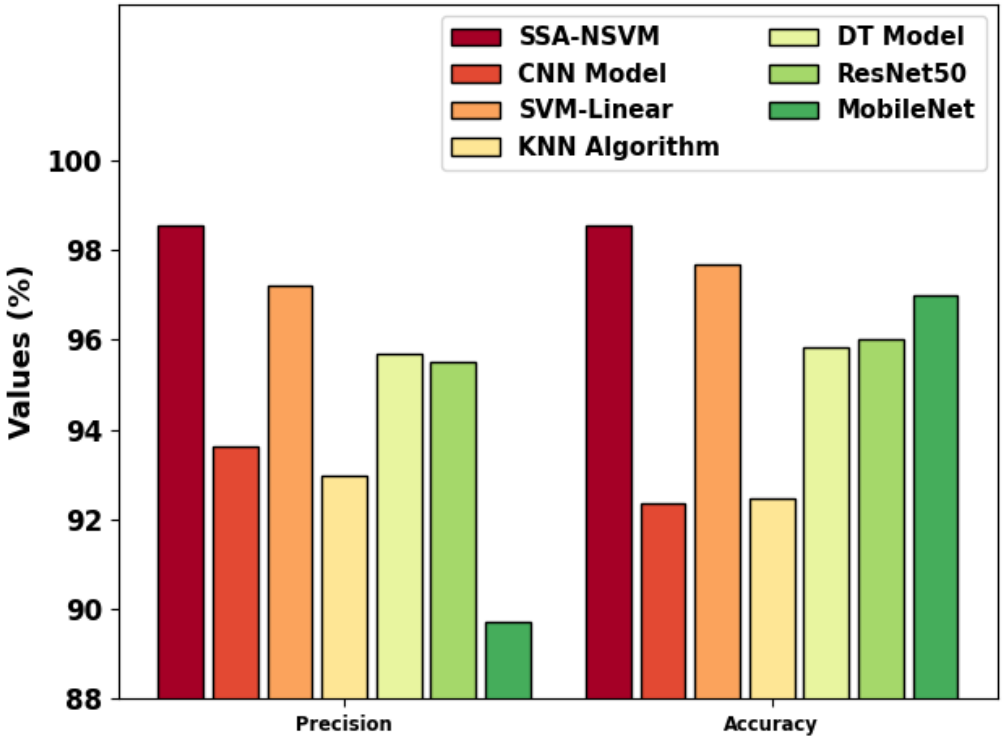

Figure 6: $Prec_n$ and $Accu_y$ analysis of SSA-NSVM technique with existing models

Doi: https://doi.org/10.54216/IJNS.230408
Received: August 02, 2023 Revised: December 04, 2023 Accepted: March 01, 2024

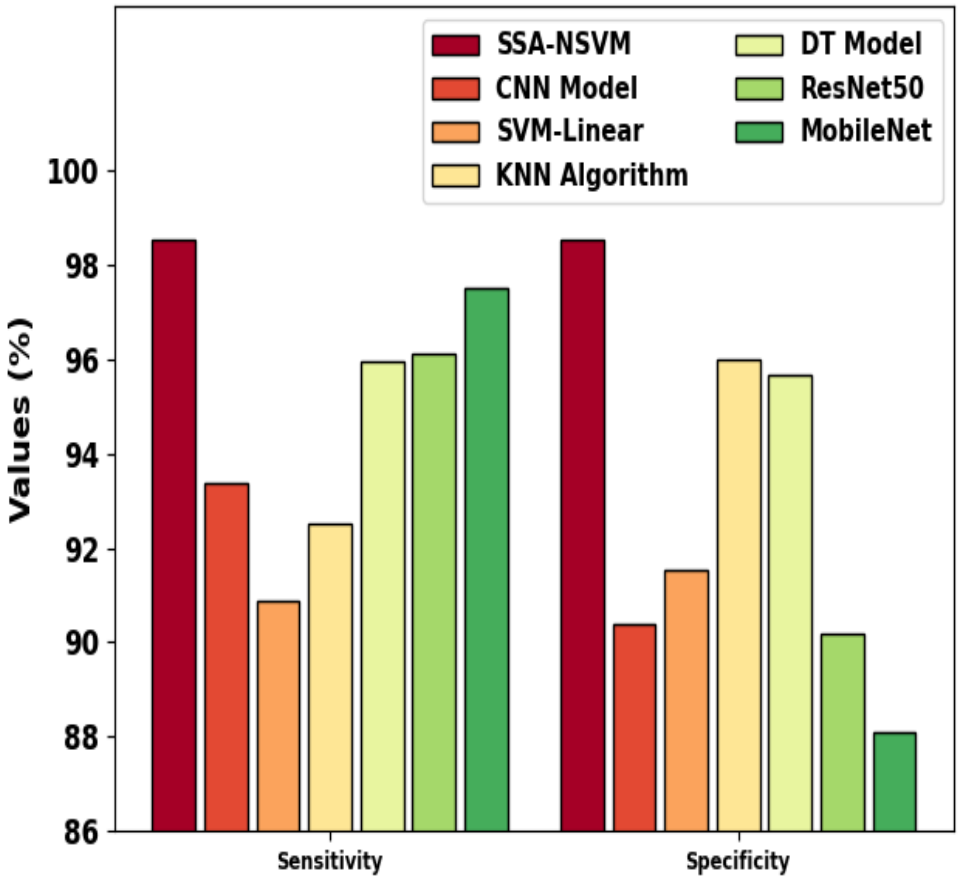

Figure 7: $Sens_y$ and $Spec_y$ analysis of SSA-NSVM technique with existing models

Fig. 7 provides a comparison analysis of the SSA-NSVM method in terms of $sens_y$ and $spec_y$. The figure demonstrated that the SSA-NSVM system gains improved performance. Based on $sens_y$, an advanced value of 98.54% is attained by the SSA-NSVM system whereas the CNN, SVM-linear, KNN, DT, ResNet, and MobileNet methodologies have described lesser $sens_y$ of 93.38%, 90.89%, 92.52%, 95.96%, 96.10%, and 97.50%, respectively. Moreover, based on $spec_y$, a greater value of 98.54% is accomplished by the SSA-NSVM method while the CNN, SVM-linear, KNN, DT, ResNet, and MobileNet systems have described lower $spec_y$ of 90.38%, 91.54%, 95.99%, 95.67%, 90.20%, and 88.10%, respectively. Therefore, the SSA-NSVM technique can be applied to the automated skin cancer classification process.

6. Conclusion

In this paper, we have established a novel SSA-NSVM model for leukemia recognition and classification. The SSA-NSVM model mainly exploits NL concepts with the DL model for the detection of leukemia. It comprises different kinds of sub-processes namely BF-based preprocessing, DenseNet-based feature extractor, SSA-based hyperparameter selection, and NSVM-based classification process. To achieve this, the SSA-NSVM methodology firstly uses BF-based image pre-processing. Furthermore, the SSA-NSVM approach utilizes a modified DenseNet system for learning complex and intrinsic feature patterns. Besides, the hyperparameter selection of the modified DenseNet model takes place using SSA. Finally, the NSVM model is employed for the detection and identification of leukemia. The performance analysis of the SSA-NSVM approach is verified by utilizing a benchmark medical image dataset. The experimental values emphasized that the SSA-NSVM method reaches better detection outcomes than other existing approaches.

Funding: "The authors extend their appreciation to the Deanship of Scientific Research at King Khalid University for funding this work through large group Research Project under grant number RGP2/462/44"

Conflicts of Interest: "The authors declare no conflict of interest."

Doi: https://doi.org/10.54216/IJNS.230408
Received: August 02, 2023 Revised: December 04, 2023 Accepted: March 01, 2024

References

[1] Ansari S et al (2023) A customized efcient deep learning model for the diagnosis of acute leukemia cells based on lymphocyte and monocyte images. Electronics 12(2):322

[2] Wolach O, Stone RM (2017) Mixed-phenotype acute leukemia. Curr Opin Hematol 24(2):139–145

[3] Laosai J, Chamnongthai K (2014) Acute leukemia classifcation by using SVM and K-Means clustering. In Proceedings of the 2014 IEEE International Electrical Engineering Congress (iEECON), Chonburi, pp. 1–4

[4] Vogado LHS, Veras RDMS, Andrade AR, De Araujo FHD, e Silva RRV, Aires KRT (2017) Diagnosing leukemia in blood smear images using an ensemble of classifers and pre-trained convolutional neural networks. In Proceedings of the 2017 IEEE 30th SIBGRAPI Conference on Graphics, Patterns and Images (SIBGRAPI), Niteroi, pp. 367–373

[5] Madhukar M, Agaian S, Chronopoulos AT (2012) Deterministic model for acute myelogenous leukemia classifcation. In Proceedings of the 2012 IEEE International Conference on Systems, Man, and Cybernetics (SMC), Seoul, pp. 433–438.

[6] Setiawan A, Harjoko A, Ratnaningsih T, Suryani E, Palgunadi S (2018) Classifcation of cell types in Acute Myeloid Leukemia (AML) of M4, M5 and M7 subtypes with support vector machine classifer. In Proceedings of the 2018 International Conference on Information and Communications Technology (ICOIACT), Yogyakarta, pp. 45–49

[7] Maurício de Oliveira J, Dantas D (2021) Classifcation of normal versus leukemic cells with data augmentation and convolutional neural networks. In Proceedings of the 16th International Joint Conference on Computer Vision, Imaging and Computer Graphics Theory and Applications (VISIGRAPP 2021) – vol. 4: VISAPP, pp. 685-692

[8] Kumar N et al (2022) Automatic Diagnosis of Covid-19 Related Pneumonia from CXR and CT-Scan Images. Eng Technol Appl Sci Res 12(1):7993–7997

[9] Prellberg J, Kramer O (2020) Acute lymphoblastic leukemia classifcationfrom microscopic images using convolutionalneural networks,arXiv:1906.09020v2 [cs.CV] 1 Apr 2020

[10] Patel N, Mishra A (2015) Automated leukemia detection using microscopic images. Procedia Comput Sci 58:635–642.

[11] Talaat, F.M. and Gamel, S.A., 2024. Machine learning in detection and classification of leukemia using C-NMC_Leukemia. Multimedia Tools and Applications, 83(3), pp.8063-8076.

[12] Sriram, G., Babu, T.R., Praveena, R. and Anand, J.V., 2022. Classification of Leukemia and Leukemoid Using VGG-16 Convolutional Neural Network Architecture. Molecular & Cellular Biomechanics, 19(2).

[13] Jha, C.K., Choubey, A., Kolekar, M.H. and Chakraborty, C., 2023. Automated Acute Lymphoblastic Leukemia Detection Using Blood Smear Image Analysis. In Machine Learning and Deep Learning Techniques for Medical Image Recognition (pp. 64-75). CRC Press.

[14] Elrefaie, R.M., Mohamed, M.A., Marzouk, E.A. and Ata, M.M., 2024. A robust classification of acute lymphocytic leukemia-based microscopic images with supervised Hilbert-Huang transform. Microscopy Research and Technique, 87(2), pp.191-204.

[15] Das, P.K., Sahoo, B. and Meher, S., 2022. An efficient detection and classification of acute leukemia using transfer learning and orthogonal softmax layer-based model. IEEE/ACM Transactions on Computational Biology and Bioinformatics.

[16] Bhute, A., Bhute, H., Pande, S., Dhumane, A., Chiwhane, S. and Wankhade, S., 2024. Acute Lymphoblastic Leukemia Detection and Classification Using an Ensemble of Classifiers and Pre-Trained Convolutional Neural Networks. International Journal of Intelligent Systems and Applications in Engineering, 12(1), pp.571-580.

[17] Sulaiman, A., Kaur, S., Gupta, S., Alshahrani, H., Reshan, M.S.A., Alyami, S. and Shaikh, A., 2023. ResRandSVM: Hybrid Approach for Acute Lymphocytic Leukemia Classification in Blood Smear Images. Diagnostics, 13(12), p.2121.

[18] Ali, M., Smarandache, F. and Vladareanu, L., 2017. Neutrosophic sets and logic. In Emerging Research on Applied Fuzzy Sets and Intuitionistic Fuzzy Matrices (pp. 18-63). IGI Global.

[19] Geng, J., Jiang, W. and Deng, X., 2020. Multi-scale deep feature learning network with bilateral filtering for SAR image classification. ISPRS Journal of Photogrammetry and Remote Sensing, 167, pp.201-213.

[20] JavadiMoghaddam, S., 2023. A novel framework based on deep learning for COVID-19 diagnosis from X-ray images. PeerJ Computer Science, 9, p.e1375.

Doi: https://doi.org/10.54216/IJNS.230408
Received: August 02, 2023 Revised: December 04, 2023 Accepted: March 01, 2024

[21] Al-Betar, M.A., Abasi, A.K., Al-Naymat, G., Arshad, K. and Makhadmeh, S.N., 2023. Bare-Bones Based Salp Swarm Algorithm for Text Document Clustering. IEEE Access.
[22] Ju, W. and Cheng, H.D., 2013. A novel neutrosophic logic svm (n-svm) and its application to image categorization. New Mathematics and Natural Computation, 9(01), pp.27-42.
[23] https://www.kaggle.com/datasets/andrewmvd/leukemia-classification
[24] Ahmed, I.A., Senan, E.M., Shatnawi, H.S.A., Alkhraisha, Z.M. and Al-Azzam, M.M.A., 2023. Hybrid techniques for the diagnosis of acute lymphoblastic leukemia based on fusion of CNN features. Diagnostics, 13(6), p.1026.

Doi: https://doi.org/10.54216/IJNS.230408
Received: August 02, 2023 Revised: December 04, 2023 Accepted: March 01, 2024